Atomistic Spin Dynamics

20

Richard F. L. Evans

Contents

Abstract

Atomistic spin models describe a class of models which approach a discrete limit of magnetic materials, where each atom is ascribed a localized atomistic magnetic moment or *spin*. These atomic spins interact principally by the Heisenberg exchange interaction, leading to long-range magnetic order and resulting in macroscopic magnetic properties. Here we review the theoretical foundations and recent developments of atomistic spin dynamics and their application to advanced magnetic materials, thermal and ultrafast spin dynamics.

R. F. L. Evans (✉)
The Department of Physics, The University of York, Heslington, York, UK
e-mail: richard.evans@york.ac.uk

© Springer Nature Switzerland AG 2020

W. Andreoni, S. Yip (eds.), *Handbook of Materials Modeling*,
https://doi.org/10.1007/978-3-319-44680-6_147

1 Introduction

The theoretical foundations of spin models were established early in the twentieth century through the discovery of the quantum mechanical property of spin (Gerlach and Stern 1924) and the formulation of the Heisenberg exchange interaction (Heisenberg 1928) giving a microscopic origin of the Weiss field (Weiss 1907). Atomistic spin models were first realized in the model of Ernst Ising (1925) which was the first attempt to formulate a description of macroscopic magnetic order from a microscopic level, which was solvable analytically. Spin models only became practically useful tools with the advent of computational physics, where the finite size properties of magnets could be studied numerically using Metropolis Monte Carlo (Metropolis et al. 1953; Binder 1969). A limitation of the Ising model is the imposition of an infinite anisotropy due to quantization of the spin direction, making it inapplicable to real magnetic materials. A generalization of the Ising model is to remove the quantization of spin and treat the atomic spins as purely classical objects, allowing them to vary freely in 3D space. This allows for more realistic simulation of magnetic materials with finite anisotropies and more complex interactions than described by a simple nearest neighbor exchange interaction, enabling Monte Carlo simulations of equilibrium properties for more realistic systems than the Ising model could describe.

With the development of general purpose computers and programming languages such as FORTRAN and C, it became possible to develop more complex algorithms and software capable of performing numerical micromagnetics. Within the micromagnetic formalism, the atomic magnetic properties are averaged over a small volume of space typically $(2–10\,\mathrm{nm})^3$ by assuming that the magnetization direction within the cell varies continuously. This approximation is known as a continuum approximation and allows the translation of the electronic properties to equivalent large scale micromagnetic equations (Fidler and Schrefl 2000). This first allowed the solution of the ground state magnetic configuration of complex magnetic structures through energy minimization and then the development of simulated magnetization dynamics by numerical solution of the Landau-Lifshitz-Gilbert equation (Fidler and Schrefl 2000). Today micromagnetics is a standard research tool due to the availability of user friendly software packages such as OOMMF and MUMAX3 and the ability to simulate relatively large structures accessible experimentally.

Despite the ubiquity of micromagnetic simulations, they are fundamentally constrained by the continuum formulation which requires that the magnetization direction varies *slowly* in space and time. This limitation means that the dynamics of ferrimagnets and antiferromagnets cannot be properly simulated since the intrinsic magnetization direction varies strongly on the atomic scale. At high temperatures the same problem exists since the thermal fluctuations lead to atomic scale spin disorder. Many technologically important materials and devices rely on ultrathin films and structures where the material properties themselves vary on the atomic length scale and cannot be properly described by the continuum approximation. Thus, the limited applicability of the micromagnetic formalism presents a barrier to understanding the dynamics of many magnetic materials and devices.

A major innovation came with the implementation of atomistic spin dynamics, where the time-dependent behavior of atomic spins is simulated using the Landau-Lifshitz-Gilbert (LLG) equation (Landau and Lifshitz 1935; Gilbert 1955). Although pioneered in the late twentieth century (Antropov et al. 1995; Krech et al. 1998), atomistic spin dynamics simulations were too computationally expensive to be practically useful until the turn of the twenty first century. The theoretical framework with an assumed classical equation of motion allowed the natural consideration of antiferromagnets and ferrimagnets (Nowak 2007), as well as atomic level defects found in nanoparticles, surfaces, and interfaces where the magnetization direction can change significantly at the atomic scale. Atomistic spin dynamics also enables the natural study of high temperature magnetization dynamics near and above the Curie temperature where the spins are paramagnetic and also spin excitations and the spin wave density of states (DOS) (Skubic et al. 2008). All of these features avoid the fundamental continuum limitation of micromagnetics and has led to a renaissance of magnetic materials modeling where the macroscopic properties of magnetic materials can be simulated using a microscopic model with a direct link to the underlying electronic properties responsible for the emergence of magnetic interactions.

2 Atomistic Spin Models

The basis of the atomistic spin model is a discrete description of magnetism, where each atom possess a localized magnetic moment or *spin*. The validity of localized spin models is often a topic of historical debate since it seems to conflict with the Stoner model of magnetism, which explains the existence of non-integer magnetic moments in metals due to the band structure. The development of first principles calculations of the spin polarized electron density revealed that in Fe and Co the electrons responsible for the magnetic moment are well localized to the nucleus and the bonding electrons tend to have only a small net spin. This supports the localized moment picture for elemental Fe and Co, while the small moment in Ni suggests that longitudinal Stoner spin fluctuations are important (Pan et al. 2017). The local moment approximation is also not well justified for induced magnetic moments such as those found in Pt and Rh in close proximity to a 3*d* magnetic metal where the spin density is distributed over the unit cell volume.

The interactions between atomistic spins are encapsulated in the spin Hamiltonian: the full Hamiltonian of the electron system with all spin-independent terms removed. A typical spin Hamiltonian $\mathscr{H}$ consisting of Heisenberg exchange, uniaxial anisotropy, and coupling to an external applied magnetic field is given by

$$\mathscr{H} = -\sum_{i<j} J_{ij}\mathbf{S}_i \cdot \mathbf{S}_j - \sum_i k_{\mathrm{u}} \left(\mathbf{S}_i \cdot \mathbf{e}_i\right)^2 - \sum_i \boldsymbol{\mu}_i \mathbf{S}_i \cdot \mathbf{B}_{\mathrm{app}}, \tag{1}$$

where i is the local atomic site, J_{ij} is the exchange interaction between spins, $\mathbf{S}_i$ is a unit vector giving the spin direction on atomic site i, $\mathbf{S}_j$ is a unit vector giving

the spin direction on a neighboring atomic site j, k_u is the uniaxial anisotropy constant on site i, $\mathbf{e}_i$ is a unit vector giving the magnetic easy axis for site i, $\boldsymbol{\mu}_i$ is the magnitude of the local atomic spin moment on site i, and $\mathbf{B}_\mathrm{app}$ is a vector describing the external applied magnetic (Zeeman) field.

In atomistic spin models, the exchange interaction is typically the strongest interaction by 2–4 orders of magnitude and is responsible for the alignment of atomic spins. In ferromagnets where $J_{ij} > 0$ this is apparent from the formation of magnetic domains which give rise to classic macroscopic magnetic behavior. In antiferromagnets where $J_{ij} < 0$, the atomic spins are aligned antiparallel, and so in weak external fields, the net magnetization is zero.

For applications the most important factor is often the magnetic stability of the material and its resistance to losing or changing its magnetic state. The stability of the material is determined by its preference for aligning along particular crystallographic orientations, a property usually known as magnetocrystalline anisotropy or magnetic anisotropy energy (MAE). The simplest form of anisotropy is uniaxial, where one magnetic axis is preferred over all others. The common magnets Fe and Ni have cubic anisotropy where the spins prefer to lie along six or eight symmetric crystal directions.

For small systems with a uniform shape such as nanoparticles, the exchange and anisotropy represent the most important interactions in the system. However, for larger systems, thin films, or elongated nanostructures, the dipole field becomes important and can dominate the magnetic structure. For a magnetic sample consisting of point dipoles, the magnetic dipole field $\mathbf{B}^i_\mathrm{dipole}$ at site i can be expressed as

$$\mathbf{B}^i_\mathrm{dipole} = \frac{\mu_0}{4\pi}\left(\sum_{i\neq j}\frac{3(\mathbf{S}_j\cdot\hat{\mathbf{r}})\hat{\mathbf{r}}-\mathbf{S}_j}{r^3}\right), \tag{2}$$

where r is the separation distance between atomic dipoles i and j and $\hat{\mathbf{r}}$ is a unit vector in the direction $i \rightarrow j$. This long-ranged interaction leads to a demagnetizing field which minimizes the surface magnetic charges. The main influence of the dipole field is shape anisotropy, where different shapes have preferred magnetic orientations. For example, thin films prefer an in-plane orientation of the magnetization or elongated nanoparticles prefer to align their magnetization along the long axis of the particle.

Numerically dipole fields represent a challenging problem since each and every dipole interacts with every other, making direct solution of Eq. 2 impossible for all but the smallest systems with a size of around 10,000 atoms or less. Therefore approximate solutions are often used treating the dipole fields with a micromagnetic approximation where the atomic magnetizations are averaged within a small volume of space (Evans et al. 2014). This allows the separation of time and length scales from the atomistic spin dynamics while incorporating the important physical effects of the demagnetizing field.

A realistic spin Hamiltonian for a specific material can invoke a number of more complex interactions, such as two-ion anisotropy (Callen and Callen 1966;

Mryasov et al. 2005), surface anisotropy (Yanes et al. 2007), Dzyaloshinskii-Moriya interactions (Dzyaloshinsky 1958; Moriya 1960), higher-order magnetocrystalline anisotropies (Skomski 2012), and higher-order four-spin terms (Barker and Chantrell 2015). These complex interactions are surprisingly common in most technologically relevant materials, but their application in spin dynamics simulations is a very recent development.

3 Spin Dynamics

While the spin Hamiltonian can describe a plethora of magnetic interactions and properties, by itself it is not especially useful. The many body problem of solving the time evolution of several interacting spins is not solvable analytically and so it is necessary to adopt classical simulations where the spin relaxation is treated adiabatically and without quantum mechanics. It is important to note however that all magnetic interactions are fundamentally quantum mechanical, and these are simply approximated as a classical potential with a classical evolution of the spin states. This allows for classical Monte Carlo simulations to calculate equilibrium thermodynamic properties, but these are unable to capture the time-dependent dynamics of the spin system. At the turn of the twenty first century, atomistic spin dynamics simulations became computationally feasible for the first time and over the past 20 years have evolved to become a standard modeling technique for magnetic materials.

The theoretical basis of spin dynamics is the time evolution of a single atomic spin given by the phenomenological Landau-Lifshitz-Gilbert (LLG) equation, first derived by Landau and Lifshitz (1935) and then extended by Gilbert to include a critical damping (Gilbert 1955). The equation incorporates a precession term which arises from the intrinsic quantum mechanical precession of spins and a relaxation term which aligns the net spin direction with an externally applied magnetic field. The LLG atomistic equation (Ellis et al. 2015) is given by

$$\frac{\partial \mathbf{S}_i}{\partial t} = -\frac{\gamma_i}{(1+\lambda_i^2)}[\mathbf{S}_i \times \mathbf{B}_i + \lambda_i \mathbf{S}_i \times (\mathbf{S}_i \times \mathbf{B}_i)], \tag{3}$$

where $\mathbf{S}_i$ is the classical spin vector of length $|\mathbf{S}_i| = 1$, $\gamma_i = 1.76 \times 10^{11}\ \mathrm{T}^{-1}\mathrm{s}^{-1}$ is the gyromagnetic ratio, λ_i is the dimensionless Gilbert damping parameter representing the coupling to the heat bath, and $\mathbf{B}_i$ is the effective magnetic field in units of tesla. At the atomistic level the, Gilbert damping is a coupling of the spin to the electronic system and lattice and as the spin precesses and leads to a loss of energy. Materials containing atoms with strong spin-orbit coupling such as Pt and Ta will typically have a high Gilbert damping (Pan et al. 2016), while insulating materials will typically have low damping. In general the lattice contribution to the Gilbert damping is weak. The effective magnetic field on each atomic spin is given by the derivative of the total spin Hamiltonian with respect to the local spin moment

plus a Langevin thermal term representing the thermal spin fluctuations (Brown 1963) and given by

$$\mathbf{B}_i = \boldsymbol{\zeta}_i(t) - \frac{1}{\mu_i}\frac{\partial \mathscr{H}}{\partial \mathbf{S}_i}, \tag{4}$$

where μ_i is the spin magnetic moment and $\boldsymbol{\zeta}_i(t)$ is a time-dependent random thermal field. The thermal fluctuations are represented by a stochastic Langevin process where the Brownian motion of the spins is simulated by a random thermal magnetic field. The statistical properties of the thermal field in time are described by a white noise process given by

$$\boldsymbol{\zeta}_i = \langle \boldsymbol{\zeta}_i^a(t)\boldsymbol{\zeta}_j^b(t)\rangle = 2\delta_{ij}\delta_{ab}(t-t')\frac{\lambda_i k_B T}{\mu_i \gamma_i}, \tag{5}$$

where

$$\left\langle \boldsymbol{\zeta}_i^a(t)\right\rangle = 0. \tag{6}$$

This stochastic Landau-Lifshitz-Gilbert equation of motion, often abbreviated to *sLLG*, describes the fundamental time dependence of classical spins in a Langevin heat bath. This enables the simulation of time-dependent phenomena and phase transitions of complex systems with an almost endless variety of fundamental interactions, properties, and structures. In particular spin waves are modeled explicitly encapsulating the essential physics of many magnetic materials at the atomic level.

The Landau-Lifshitz-Gilbert equation is the essential equation describing magnetization dynamics from atomic to micromagnetic and macroscopic length scales. The development of numerical micromagnetics required numerical solution of the LLG equation and over the years has attracted a wide range of numerical schemes including simple predictor-corrector methods, Runge-Kutta, semi-implicit, midpoint, and symplectic integration schemes. For micromagnetics the effective magnetic fields in the LLG equation are generally small (a few Tesla) and slowly varying and so the integration is essentially limited by the ability to exactly conserve the magnetization length during integration. For atomistic spin dynamics, the requirements are somewhat different since the exchange fields are large (typically 100–1000 T), and the thermal fluctuations are of a similar magnitude at high temperatures due to the atomic values of the spin moment. This firstly requires a numerical integration scheme that leads to the Stratonovich interpretation of the stochastic LLG equation, such as the Heun scheme (García-Palacios and Lázaro 1998). Secondly small time steps around 0.1 fs are required to correctly resolve the dynamics of the spins. This is because spin excitations at elevated temperatures and in ferrimagnets and antiferromagnets are especially large, leading to a rapidly changing effective field in both magnitude and direction. The rapidly changing field means that the fundamental dynamics are not limited by the numerical integration scheme but by the physics of spin dynamics at the atomic scale. Practically this means that there is no value in integration schemes more complex than Heun due to their higher numerical cost. Alternative approaches such as pulsed noise (Garanin

2017) may alleviate some of the problems with large spin excitations and allow larger time steps, but it is not yet clear that this is beneficial for antiferromagnets where the dynamics are intrinsically on the femtosecond timescale.

3.1 Quantum Statistics

In the above classical treatment, all quantum mechanical variables have been replaced with classical variables. The presence of a Langevin thermostat means that infinitesimal changes to spin orientations are allowed. In reality of course spin, transitions are discrete and caused by spin-flip scattering processes induced by incoming photons or electrons interacting with the spins. This means that there is a natural gap in the spectrum where low energy electron and photon excitations are unable to cause a spin flip. This behavior naturally leads to quantum statistics, where there are distinct spin energy levels that are populated. This can be represented in a spin model by considering the intensity of thermal fluctuations and changing their intensity to give the expected magnon distribution (Bergqvist and Bergman 2018) or parametrically by rescaling the effective temperature in the simulation (Evans et al. 2015) to give the experimentally measured temperature-dependent magnetization, which is a direct estimate of the magnon population. However, this still avoids the fundamental nature of the underlying microscopic spin-flip processes. Therefore, the thermodynamic properties of magnetic materials are only approximate and pure classical spin models typically give an incorrect temperature-dependent magnetization curve due to the classical nature of the statistics of the thermal bath.

4 Advanced Models of Magnetic Materials

Simple spin models are based on a straightforward extension of finite difference micromagnetics to atomic resolution, where each cell is the size of an atom and the continuum micromagnetic interactions are replaced with their discrete equivalents with a simple cubic lattice. While these models are qualitatively useful in describing thermal effects and atomic scale magnetism, they suffer from a weak relation to reality where the atomic structure, electronic properties, and magnetism interplay to give a complex range of magnetic phenomena in a wide diversity of magnetic materials. To better understand the magnetic properties with a high degree of specificity, it is necessary to formulate a realistic model of a material including the correct crystal structure and a realistic model of the magnetic interactions. Examples of atomistic spin models of specific materials include FePt (Mryasov et al. 2005), GdFe alloys (Ostler et al. 2011), Fe_3O_4 (Nedelkoski et al. 2017), FeRh (Barker and Chantrell 2015), YIG (Barker and Bauer 2016), $Nd_2Fe_{14}B$ (Toga et al. 2016), and IrMn (Szunyogh et al. 2009; Yanes et al. 2013), where the structure and magnetic interactions are included explicitly in the model. For atomistic spin models, such material-specific models are a relatively recent development, starting

around 20 years ago. In the future such models will be essential to fully understand the fundamental and thermodynamic properties of magnetic materials.

4.1 Amorphous GdFe Alloys

One of the main advantages of atomistic spin models over micromagnetics is the ability to correctly simulate the dynamics of ferrimagnetic and antiferromagnetic materials. In these materials, the localized atomic spins are exchange coupled in an antiparallel state. The partial or complete compensation of the magnetization at the atomic level leads to inertial spin dynamics with a rich variety of behavior making them particularly interesting at the fundamental level as well as practically important. Technologically one of the most important ferrimagnetic materials is GdFe, an amorphous alloy of the rare earth (RE) metal Gd and transition metal (TM) Fe. Here the Gd and Fe atoms form two magnetic sublattices that oppose each other and due to the different origin of the magnetic moments, *4f* and *3d* electrons, respectively. The Fe atoms draw their magnetic moments from the *3d* electrons, and the spin polarized electron density is quite well localized near the nucleus with an effective spin magnetic moment of $1.92\,\mu_B$ per atom. The Gd atoms have a magnetic moment due to the *4f* electron shell, which is lower in energy than the *6s* and *5d* shells and prefers unpaired filling of the orbitals. This leads to a large effective spin moment of $7.63\,\mu_B$ per atom. Since the *4f* electron shell is located away from the *5d* bonding electrons, the exchange coupling is weaker than in the transition metal elements, leading to a lower Curie temperature of 298 K for pure Gd metal. However, when alloyed together as GdFe, the effective Curie temperature is around 500 K which is sufficiently above room temperature to be useful for applications such as magneto-optical recording. This is because the exchange interaction from the Fe sublattice polarizes the Gd spin moments causing an increase in the effective exchange interaction and thus the Curie temperature for the coupled system.

It is possible to model the static and dynamic properties of GdFe alloys using an extended spin model explicitly considering Fe and Gd spin moments and Heisenberg exchange coupling (Ostler et al. 2011). Experimentally GdFe alloys are assumed to be amorphous where the Fe and Gd atoms are almost homogeneously distributed in the material with no short-range or long-range crystallographic order. This would add a significant degree of complexity to the simulations, with a wide range of exchange interaction strengths, coordination number, and density fluctuations. The simplest approach is to consider a magnetically amorphous material where the Gd and Fe sites are randomly distributed within a periodic crystal structure which captures the essence of the magnetic interactions and ferrimagnetic properties. Alloys used for magneto-optical recording applications typically have a composition close to $Gd_{25}Fe_{75}$ to balance the requirement for a low Curie temperature and larger magnetic moment when heating the material to enable recording of information. In thin film form when sandwiched between SiN glass, GdFe films have a strong perpendicular magnetic anisotropy, usually assumed to arise due to interfacial or surface anisotropy. Having defined the interactions in the systems, we can write down the spin Hamiltonian

$$\mathscr{H} = \mathscr{H}_{\mathrm{Gd}} + \mathscr{H}_{\mathrm{Fe}} \tag{7}$$

$$\mathscr{H}_{\mathrm{Gd}} = -\sum_{i<j} J_{\mathrm{Gd}} \mathbf{S}_i \cdot \mathbf{S}_j - \sum_{i<\delta} J_{\mathrm{GdFe}} \mathbf{S}_i \cdot \mathbf{S}_\delta - \sum_i k_{\mathrm{u}} \left(\mathbf{S}_i \cdot \mathbf{e}_i\right)^2 - \boldsymbol{\mu}_{\mathrm{Gd}} \sum_i \mathbf{S}_i \cdot \mathbf{B}_{\mathrm{app}} \tag{8}$$

$$\mathscr{H}_{\mathrm{Fe}} = -\sum_{\nu<\delta} J_{\mathrm{Fe}} \mathbf{S}_\nu \cdot \mathbf{S}_\delta - \sum_{\nu<j} J_{\mathrm{GdFe}} \mathbf{S}_\nu \cdot \mathbf{S}_j - \sum_\nu k_{\mathrm{u}} \left(\mathbf{S}_\nu \cdot \mathbf{e}_\nu\right)^2 - \boldsymbol{\mu}_{\mathrm{Fe}} \sum_\nu \mathbf{S}_\nu \cdot \mathbf{B}_{\mathrm{app}} \tag{9}$$

which explicitly lists inter-sublattice ($J_{\mathrm{GdFe}} = -1.09 \times 10^{-21}$ J/link) and intra-sublattice ($J_{\mathrm{Gd}} = 1.26 \times 10^{-21}$ J/link and $J_{\mathrm{Fe}} = 2.835 \times 10^{-21}$ J/link) exchange interactions and different couplings to the applied field (Ostler et al. 2011). The anisotropy is assumed to be uniaxial due to the surface effect of SiN capping layers used in experiments with a value of $k_{\mathrm{u}} = 8.07246 \times 10^{-24}$ J/atom. The form given here is encapsulated in the simplified form in Eq. 1 but is more specific in identifying relevant sets of interactions and values in the system.

Having defined the interactions in the system, it is then possible to simulate the equilibrium temperature-dependent properties using atomistic spin dynamics. Figure 1 shows the calculated temperature dependence of the equilibrium sublattice and total magnetizations and reproduces the main features of the material seen experimentally: a magnetic compensation point and different temperature-dependent magnetizations of the Fe and Gd sublattices (Ostler et al. 2011). It is important to note that the two magnetic sublattices in GdFe have the same Curie temperature, while their different temperature dependencies come from the different intrinsic exchange interactions, being much weaker for Gd spins compared with Fe. At the compensation point, the net magnetization is close to zero and so macroscopically the system of spins behaves like an antiferromagnet. The existence of a compensation point is only possible due to the different temperature dependences of the Fe and Gd sublattices. This arises because the Gd spins are polarized by the exchange interaction from neighboring Fe spins, which leads to order in the Gd sublattice above its intrinsic Curie temperature of 298 K. However, the spin fluctuations on the Gd sites are larger than the Fe sites due to the lower total exchange, which significantly reduces the Curie temperature of the combined system.

4.2 Magnetite

Magnetite is the oldest known magnetic material, first documented by the ancient Greeks and known in medieval times as lodestone and used as a primitive compass. Despite its long history, the origins of its magnetism are still an active subject of investigation. Magnetite is an oxide of iron with formula unit Fe_3O_4 and has a complex inverse spinel crystal structure, as shown in Fig. 2. The structural

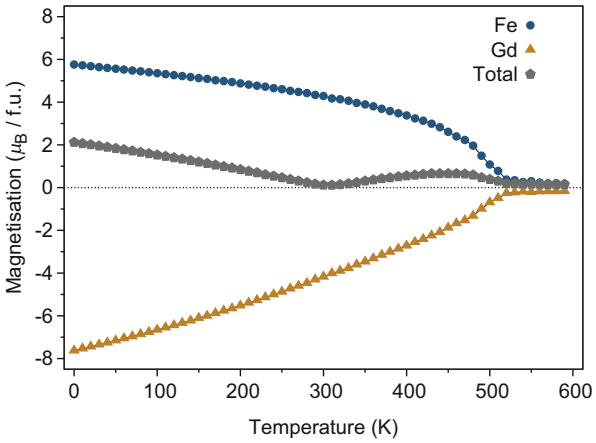

Fig. 1 Plot of the simulated sublattice temperature-dependent magnetization of $Gd_{25}Fe_{75}$ random alloy showing the effect of increased spin fluctuations on the total magnetization. The polarizing effect of the Fe spins on the Gd spins leads to a different temperature dependence of the magnetization as seen from the shape of sublattice magnetization curves. The Fe sublattice exhibits a typical classical $M_s(T)$ curve showing critical behavior near the Curie temperature T_C, while the Gd sublattice shows an almost linear behavior. The ferrimagnetic nature of the exchange coupling between the sublattices and the different temperature-dependent magnetizations naturally leads to a magnetic compensation point where the net magnetization is close to zero. The compensation point leads to a range of complex behaviors due to the inertial magnetization dynamics

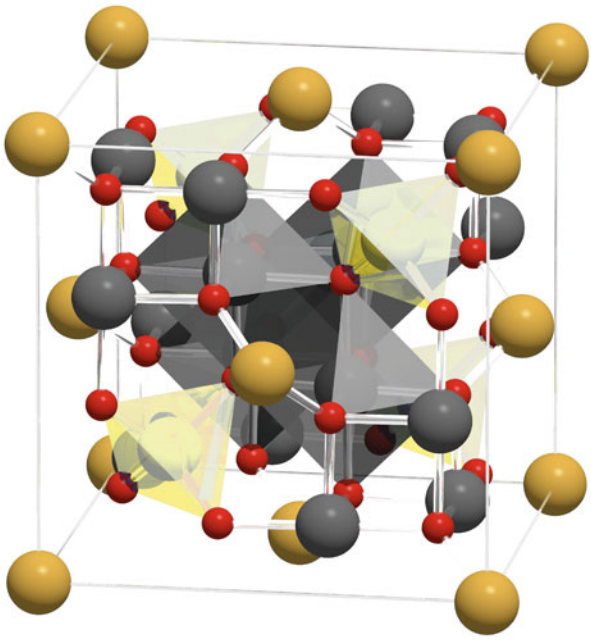

Fig. 2 Visualization of the inverse spinel crystal structure of magnetite (Fe_3O_4) showing the different magnetic site symmetries. (Image courtesy of Daniel Meilak)

complexity is typical of the vast majority of magnetic materials and represents a recent development in materials modeling where the structural and magnetic properties are strongly related and must be properly represented in the simulations. In the case of magnetite, the exchange interactions between Fe sites arise due to the double exchange interaction mediated by the oxygen atoms where its strength is determined by the relative overlap of the atomic orbitals. The crystal structure of magnetite contains two distinct sites based on the local oxygen symmetry: tetrahedral and octahedral. The site symmetries define two distinct magnetic sites with different coordination number and localized magnetic moments on the Fe ions due to the different valence states of the Fe. Expanding the spin Hamiltonian into these components we therefore have

$$\mathscr{H} = \mathscr{H}_{\mathrm{Fe}}^{\mathrm{T}} + \mathscr{H}_{\mathrm{Fe}}^{\mathrm{O}} \tag{10}$$

$$\begin{aligned}\mathscr{H}_{\mathrm{Fe}}^{\mathrm{T}} = &-\frac{1}{2}\sum_{i,j} J_{\mathrm{Fe}}^{\mathrm{TT}} \mathbf{S}_i \cdot \mathbf{S}_j - \frac{1}{2}\sum_{i,\delta} J_{\mathrm{Fe}}^{\mathrm{TO}} \mathbf{S}_i \cdot \mathbf{S}_\delta \\ &-\frac{k_{\mathrm{c}}}{2}\sum_{i}\left(S_x^4 + S_y^4 + S_z^4\right) - \mu_{\mathrm{Fe}}^{\mathrm{T}} \sum_{i} \mathbf{H}_{\mathrm{app}} \cdot \mathbf{S}_i \end{aligned} \tag{11}$$

$$\begin{aligned}\mathscr{H}_{\mathrm{Fe}}^{\mathrm{O}} = &-\frac{1}{2}\sum_{\nu,\delta} J_{\mathrm{Fe}}^{\mathrm{OO}} \mathbf{S}_\nu \cdot \mathbf{S}_\delta - \frac{1}{2}\sum_{\nu,j} J_{\mathrm{Fe}}^{\mathrm{TO}} \mathbf{S}_\nu \cdot \mathbf{S}_j \\ &-\frac{k_{\mathrm{c}}}{2}\sum_{\nu}\left(S_x^4 + S_y^4 + S_z^4\right) - \mu_{\mathrm{Fe}}^{\mathrm{O}} \sum_{\nu} \mathbf{H}_{\mathrm{app}} \cdot \mathbf{S}_\nu, \end{aligned} \tag{12}$$

where T and O indicate tetrahedrally coordinated and octahedrally coordinated Fe ions, respectively. The exchange coupling constants $J_{\mathrm{Fe}}^{\mathrm{TT}} = -2.2 \times 10^{-22}$ J/link, $J_{\mathrm{Fe}}^{\mathrm{TO}} = -5.256 \times 10^{-21}$ J/link, and $J_{\mathrm{Fe}}^{\mathrm{OO}} = -1.0206 \times 10^{-21}$ J/link represent the super exchange interactions between the tetrahedrally and octahedrally coordinated spins. Magnetite exhibits cubic crystal symmetry and so cubic magnetocrystalline anisotropy is included at each Fe site where $k_{\mathrm{c}} = 8.16 \times 10^{-25}$ J/atom is the effective cubic anisotropy at room temperature. Due to the double exchange interaction, the leading term $J_{\mathrm{Fe}}^{\mathrm{TO}}$ is antiferromagnetic which causes magnetite to be ferrimagnetic with opposed tetrahedral and octahedral magnetic sublattices. Unlike GdFe there is no magnetic compensation point in magnetite as the sublattices have a similar temperature dependence.

5 Applications of Spin Dynamics

The core methodology of spin dynamics has been established for over 20 years, but its usefulness at that time was previously limited by a lack of fundamental materials knowledge and the computational expense of modeling reasonably sized systems with simple serial codes. Materials knowledge has advanced considerably

in that time, in particular new capabilities of first principles methods such as the Korringa-Kohn-Rostoker (KKR) method and conventional relativistic density functional theory (rDFT) to determine magnetic properties and parameters and map them to an effective Heisenberg model. The development of parallel spin dynamics codes such as VAMPIRE (https://vampire.york.ac.uk) and UPPASD (http://physics.uu.se/forskning/materialteori/pagaende-forskning/uppasd/) has enabled the simulation of much larger systems than previously possible, using thousands of cores for large-scale simulations at sizes comparable with micromagnetics. These improvements have enabled spin dynamics simulations to address fundamental challenges in magnetic materials modeling in a wide range of applications including heat-assisted magnetic recording (HAMR), magnetic random access memory (MRAM), nanoparticle magnetism, ultrafast magnetism, permanent magnets, and spintronics. It is impossible to cover the full range of applications in the present chapter, but to give a flavor of the capabilities of spin dynamics, we illustrate a few topical examples from slow to ultrafast magnetic processes.

5.1 Calculation of the Effective Gilbert Damping

The Gilbert damping parameter describes the ability of a magnetic material to respond to a magnetic field. The intrinsic damping is mainly electronic in origin (Pan et al. 2016) arising from spin-orbit coupling. However, real materials are often far from ideal and exhibit enhanced damping due to defects and impurities. Another important origin of enhanced damping is caused by thermal spin fluctuations, more commonly known as spin wave scattering. These extrinsic contributions to damping can be modeled directly using spin dynamics by performing a simple magnetic relaxation experiment. The idea is to simulate the relaxation of the net magnetization $\mathbf{M}$ toward a magnetic field $\mathbf{B}_{\text{app}}$ after performing an arbitrary rotation of the spin direction by an angle θ. Since the dynamics of the total magnetization follows the Landau-Lifshitz-Gilbert equation which has an analytical solution (Evans et al. 2014), it is possible to extract an effective damping constant from the simulation by fitting to the time-dependent relaxation of the net magnetization.

Here we consider a simple ferromagnetic $(10\,\text{nm})^3$ cube of α-Fe with zero magnetocrystalline anisotropy. The effect of spin fluctuations on the damping is calculated by simulating the time-dependent relaxation of a small block of material. The system is first equilibrated at the simulation temperature to thermalize the spins in a strong field. The net magnetization of the system is then instantaneously rotated to an angle of 30 degrees to the applied field direction which causes the net magnetization to precess around the field and gradually relax toward the field direction. Since the microscopic and macroscopic equations of motion are the same, in the absence of spin fluctuations, the input and calculated damping are expected to be the same. The ability to extract the effective Gilbert damping from the simulation requires that applied magnetic field is much larger than the equivalent anisotropy field; otherwise, the spin-dependent fields lead to a large error in the fitting. Zero anisotropy removes any restrictions on the field which can be used,

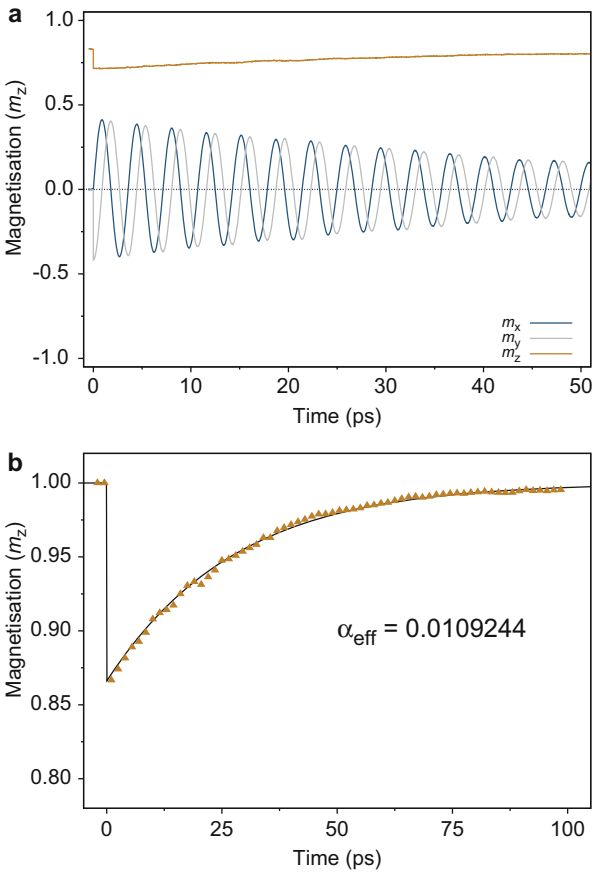

Fig. 3 (**a**) Plot of the simulated magnetization dynamics of a $(10\,\text{nm})^3$ block of α-Fe at $T = 800\,\text{K}$ in a 10 T applied field after an instantaneous rotation of the magnetization to 30° from the field direction. The rotation causes the magnetization to precess around the field direction and relax toward the applied field direction. The intrinsic Gilbert damping at $T = 0\,\text{K}$ is $\alpha = 0.01$. (**b**) Fitting of the normalized z-component of the magnetization from the analytic solution (Evans et al. 2014). The effective damping shows a small enhancement due to thermal spin fluctuations at elevated temperatures

while for materials with a large anisotropy, much larger fields can be applied. The result of the relaxation simulation for a 10T applied field and intrinsic damping of $\lambda = 0.01$ is shown in Fig. 3 for a temperature of 800 K, a significant fraction of the Curie temperature of 1048 K where spin fluctuations are relatively large. The lines show a fit to the analytic solution incorporating a phase shift due to the initial starting angle of the magnetization of 30° from the applied field direction. Here the thermal spin fluctuations lead to a small increase in the effective damping of around 10%. Modeling other contributions to the Gilbert damping is at an early stage, but spin-lattice dynamics offer an enticing route to understanding spin-phonon

interactions, particularly in magnetic oxides such as yttrium iron garnet ($Y_3Fe_5O_{12}$) and magnetite (Fe_3O_4) where the electronic damping is small.

5.2 Magnetization Dynamics in Fe_3O_4 Nanoparticles

An important property of nanoparticles is superparamagnetism, where the thermal fluctuations are sufficiently strong to make the magnetization direction of the particle unstable. The magnetocrystalline anisotropy of magnetite is relatively small, and so superparamagnetism is a common feature of nanoparticles in the 5–15 nm size range typically used for applications in magnetic hyperthermia. Using atomistic spin dynamics, we are able to directly simulate the thermodynamic properties of small magnetite nanoparticles. Using the model of magnetite described earlier, we can build an idealized single-crystal magnetite nanoparticle with an octahedral particle geometry, as shown in Fig. 4. The particle faceting is representative of experimental samples where [111] facets are energetically favorable.

The dynamics of the particle are simulated for a total of 10 ns, but even over this very short timescale, the magnetization is found to be unstable. Due to the cubic magnetocrystalline anisotropy the, minimum energy directions are along the [111] crystal directions. This can be seen from the simulations since the magnetization fluctuates in three dimensions between these eight minima. Extended calculations such as these provide detailed information about the relaxation rates of the particles which is important for other modeling techniques which assume a particular relaxation attempt frequency. Spin dynamics simulations enable this important

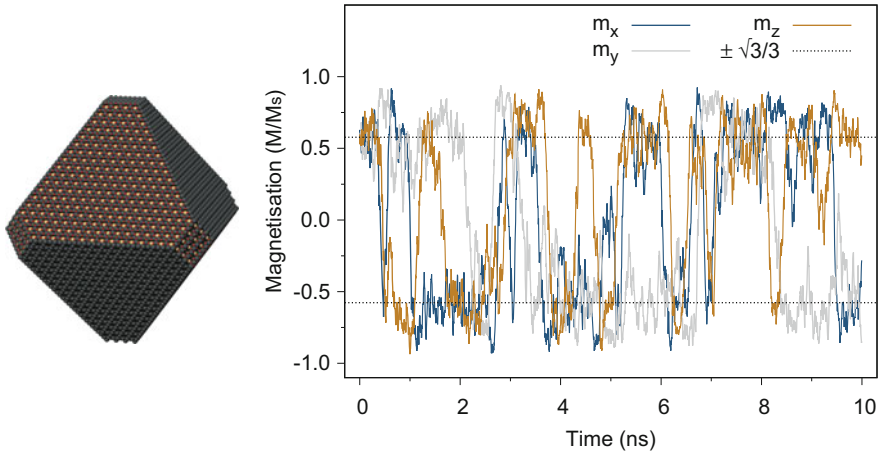

Fig. 4 Visualization of a 12 nm Octahedral magnetite nanoparticle (left) and plot of the simulated time-dependent magnetization dynamics at $T = 300$ K (right). The data show fluctuations of the different magnetization components between the 8 minima along the [111] crystal directions due to the cubic magnetocrystalline anisotropy, indicated by the dashed lines

property to be directly simulated for a range of situations such as enhanced surface anisotropy or in the presence of defects such as antiphase boundaries (Nedelkoski et al. 2017).

5.3 Ultrafast Demagnetization of Ni

The dynamics of magnetic materials were once thought to be slow, and limited by the precession frequency of a magnetic spin in a field, given by the Larmor frequency $\omega = -\gamma|\mathbf{B}|$, where $\gamma = 1.76 \times 10^{11}$ $\mathrm{T}^{-1}\mathrm{s}^{-1}$ is the gyromagnetic ratio and $|\mathbf{B}|$ is the applied magnetic field strength. For everyday magnetic field strengths of around 1 T and where the Gilbert damping is included, this gives a characteristic precession time $\tau_p = -2\pi(1+\alpha^2)/(\gamma|\mathbf{B}|)$ of around 70 picoseconds (70×10^{-12} s). The relaxation time is a multiple of the precession time $\tau_r = \tau_p/\alpha$, where the magnetization has to reorient itself with an external magnetic field. For critical Gilbert damping $\alpha = 1$, the relaxation time is the same as the precession time. However most magnetic materials have much lower damping between 0.001 and 0.1 leading to dynamics on the nanosecond timescale.

In 1996, pioneering experiments showed that metallic Ni responded to a femtosecond laser pulse on the sub-picosecond timescale (Beaurepaire et al. 1996). At the time this was a controversial discovery since it shows magnetic relaxation three orders of magnitude faster than the intrinsic relaxation time from the known properties of magnets. The ultrafast relaxation is caused by thermal spin fluctuations induced through rapid laser heating, though the microscopic mechanism responsible for the transfer of angular momentum from the spins is still debated. At the time the transfer of energy to the spins was described with a simple phenomenological three-temperature (3TM) model (Kirilyuk et al. 2010). The model describes the coupling of electron, lattice, and spin systems as reservoirs for energy. The laser pulse interacts directly with the electrons in the material causing a large increase in their thermal energy. Over the course of a few picoseconds, the hot electrons interact with the lattice causing an increase in the lattice temperature. The heat capacity of the electron system is quite small and so the electron system reaches a much high temperature than the lattice. In a magnetic material, the spins act as another reservoir which can exchange energy with the electrons and lattice. Atomistic spin dynamics is able to simulate this thermal energy transfer directly by calculating the effect of rapid heating, where it can be assumed that the hot electrons interact directly with the 3*d* spins in the material. In this case one can use the two-temperature model to simulate the dynamic response of the electron and lattice temperatures to the laser pulse. This is expressed by the coupled equations

$$\left(T_\mathrm{e} C_\mathrm{e} \frac{\partial T_\mathrm{e}}{\partial t}\right) = -G_\mathrm{el}\left(T_\mathrm{e} - T_\mathrm{l}\right) + P(t) \tag{13}$$

$$C_\mathrm{l} \frac{\partial T_\mathrm{l}}{\partial t} = G_\mathrm{el}\left(T_\mathrm{e} - T_\mathrm{l}\right), \tag{14}$$

where T_e is the electron temperature, C_e is the electron heat capacity, G_{el} is the electron-lattice coupling, T_l is the lattice temperature, C_l is the lattice heat capacity, and $P(t)$ is a time-dependent energy source from the laser heating. The electron heat capacity is assumed to scale with the electron temperature, known as the free electron approximation. The laser heating is assumed to have a Gaussian profile in time $P(t)$ given by

$$P(t) = \frac{P_0}{\sqrt{2\pi}} \exp\left(\frac{-(t-t_0)}{t_p^2}\right), \tag{15}$$

where P_0 is the laser power, t_p is the pulse width, t is the time, and t_0 is the arrival time of the pulse. These equations can now be solved numerically to determine the response of the electron and lattice temperatures of a Ni surface to a 50 fs laser pulse. A typical time evolution is shown in Fig. 5a. The smaller heat capacity of the electron leads to a large transient increase in the electron temperature caused by the laser energy. After a few hundred femtoseconds, the electron system begins to transfer energy to the lattice which causes a slower increase in the lattice temperature. The final equilibrium temperature of the system is much lower than the peak electron temperature due to the much larger heat capacity of the lattice.

We now simulate the effect of this transient temperature rise caused by the laser pulse on the magnetization of Ni by coupling the $3d$ spins to the electron temperature. We simulate the effect by considering a small segment of the Ni film $(10\,\text{nm})^3$ with periodic boundary conditions in the $x-y$ plane. The response of the z-component of the magnetization is shown in Fig. 5b. Initially before the pulse, the magnetization shows incomplete magnetic order due to the natural thermal spin fluctuations at an ambient temperature of 300 K. When the laser pulse arrives, there is a rapid decrease in the magnetization due to the rapid temperature rise. This causes large thermal spin fluctuations at the atomic level and observed as a transient decrease in magnetic order. A snapshot visualization of the spins during the maximum demagnetization is shown in Fig. 5c. During this process the net angular momentum is transferred to the lattice by electron-lattice interactions. After the pulse has gone, the reduction in the electron temperature leads to a recovery of the magnetization on a longer timescale than the initial demagnetization process. At longer timescales the magnetization reaches a new equilibrium value due to the deposition of heat in the sample by the laser pulse.

Through spin dynamics simulations, we are therefore able to model and understand the basic thermalization process of spins due to laser heating. However, this leaves several outstanding questions. The light matter interactions are complex due to the intensity of the pulse, leading to transient changes of the electronic structure and ultrafast spin currents that are not included within the simple approach above. Also the model completely neglects the underlying spin-flip scattering processes that are responsible for the microscopic spin fluctuations and angular momentum transfer. For the first few fs, the fundamental magnetic parameters are also strongly time and temperature dependent due to the effects of the laser on the underlying

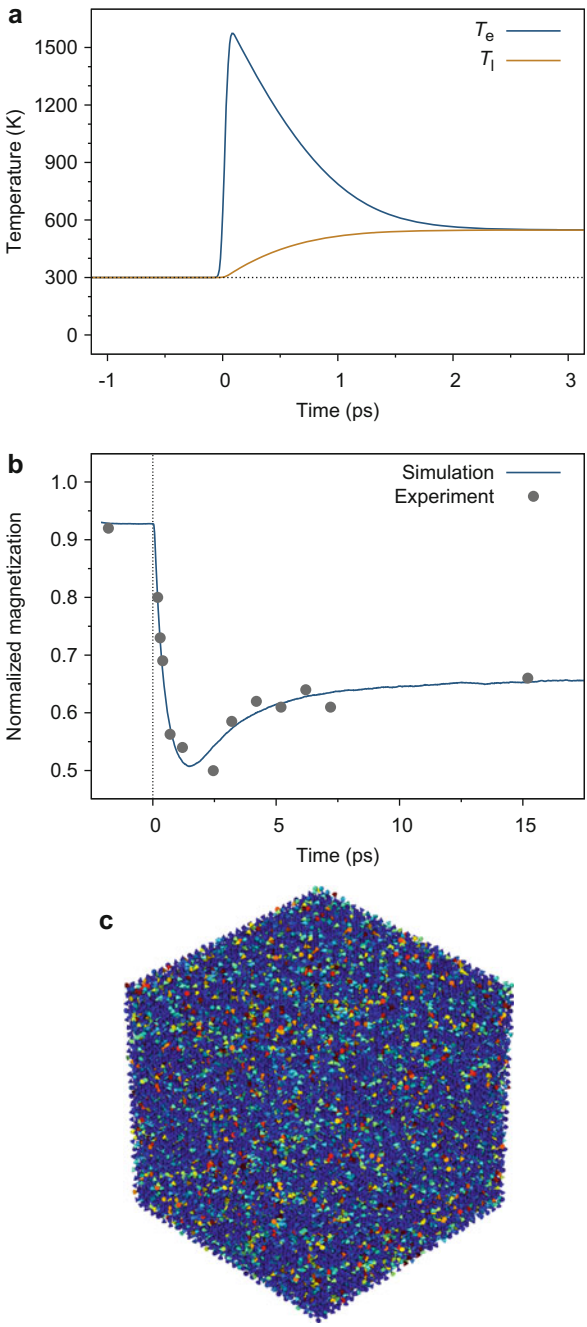

Fig. 5 (**a**) Plot of the simulated time dependence of the electron and lattice temperatures from numerical solution of the two-temperature model. (**b**) Simulated transient magnetization dynamics of a $(10\,\text{nm})^3$ block of Ni excited by a 50 fs laser pulse. The simulations show excellent agreement with experimental measurements (Beaurepaire et al. 1996). (**c**) Visualization of the spin configuration during demagnetization showing thermalization of the spins

electronic structure (Simoni et al. 2017). This makes the field of ultrafast magnetism one of the most exciting areas of the field today and will almost certainly lead to huge advances in our understanding of magnetic processes at the fundamental atomic level.

5.4 Heat-Induced Switching of GdFe

In the previous section, the thermalization of spins described the demagnetization of Ni. More recently the ability to completely control magnetic order just with light was demonstrated in amorphous GdFe (Stanciu et al. 2007). Here pulses of circularly polarized light were able to change the direction of the magnetization, rather than just demagnetization. At the time this was thought to be due to the inverse Faraday effect which induces a net angular moment from the circular polarization of the light. However, further investigation of the sublattice magnetization dynamics with X-ray magnetic circular dichroism (XMCD) and complementary modeling with atomistic spin dynamics (Radu et al. 2011) showed a complex switching mechanism where the Fe and Gd sublattice magnetizations demagnetized at different rates and at some point are aligned in parallel, despite the strong antiferromagnetic coupling between them. These complex dynamics were confirmed by atomistic spin dynamics simulations (Radu et al. 2011) and showed that angular momentum transfer was an important component of the switching process. During the course of this work, the spin dynamics simulations made a startling prediction that the reversal occurred in the absence of a magnetic fields and linearly polarized laser light, essentially *heat* induced magnetic switching. This was possible due to the realistic model of the GdFe material that had been developed, explicitly including the dynamics of Fe and Gd sublattices and their response to an ultrafast heat pulse. This remarkable prediction was confirmed experimentally (Ostler et al. 2012) through laser heating and more recently through pure hot electron transport (Yang et al. 2017), confirming that ultrafast heating alone is sufficient to cause magnetic switching in GdFe.

We will now reproduce this predictive result with a spin dynamics simulation, combining the earlier GdFe model with an ultrafast heat pulse. The model parameters are unchanged apart from a more realistic value of the Gilbert damping of $\lambda = 0.1$ since we are interested in reproducing realistic dynamics rather than equilibrium properties. The response of the system to the heat pulse is shown in Fig. 6. As with the Ni simulation earlier, the initial magnetization shows reduced order before the pulse due to thermal spin fluctuations. When then laser pulse arrives, the transient increase in the electron temperature causes rapid demagnetization of the Fe and Gd sublattices due to the heating. However, due to the different local atomic magnetic moments, the demagnetization times are different for each sublattice. This is because the larger magnetic moments on the Gd sites are less strongly affected by thermal fluctuations responsible for demagnetization. This in turn affects the magnetization dynamics, making the Gd sublattice slow to respond to the laser heating pulse. At the same time, the Fe sublattice fully demagnetizes. After the

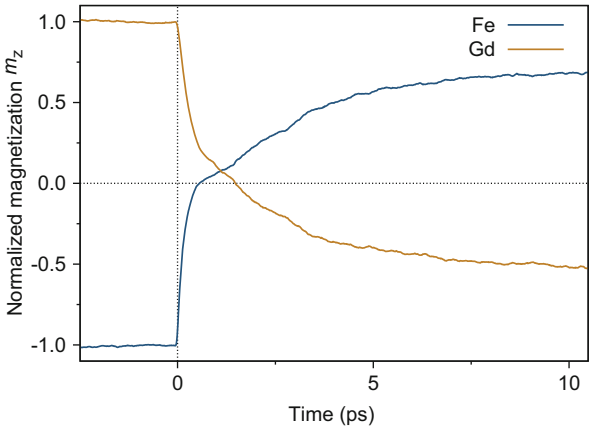

Fig. 6 Simulated heat-induced magnetic switching of GdFe be 50 fs laser pulse

pulse is gone, the system attempts to re-magnetize, but the exchange field from the partially demagnetized Gd sublattice causes the Fe sublattice to precess rapidly. The Fe precession excites a mutual precession of the Gd sublattice which leads to a dynamic switching process. A fraction of a picosecond later, the magnetization recovers sufficiently to cause the sublattices to align with the magnetic easy axis, completing the switching process (Atxitia et al. 2013). After cooling back to ambient temperature and pulsing again, this process is repeatable and deterministic. This concisely demonstrates the predictive power of atomistic spin dynamics simulations which will only improve over the coming years.

6 The Future

Despite the impressive capabilities of spin dynamics simulations, significant challenges remain in being able to fully understand the dynamics of magnetic materials both in terms of atomic structure and magnetic properties. A new class of model has recently emerged which couples spin and molecular dynamics in a single simulation (Ma et al. 2008; Perera et al. 2016, 2017). This allows an investigation of spin-lattice effects in a direct manner including contributions to the Gilbert damping and magneto volume effects, where the magnetic properties are linked to the lattice parameter. Such models are more computationally expensive than spin models but offer significant improvements in our ability to understand the dynamic properties of magnetic materials.

Another more fundamental limitation of the classical Heisenberg model is the use of classical statistics for the Langevin heat bath. In reality the underlying microscopic mechanisms are discrete electron excitations, causing small jumps in the local spin direction. This process is much better represented by quantum statistics, where infinitesimal spin fluctuations are forbidden. For larger ensembles

of spins, the temperature rescaling method includes an average effect of the lack of infinitesimal spin states by including smaller thermal fluctuations. However, smaller systems such as molecular magnets or isolated spins will require a better treatment of spin fluctuations and single spin dynamics.

Another class of magnetic moment not well treated by a fixed spin approximation induced magnetic moments or moments that are more Stoner-like rather than Heisenberg-like, where their length varies significantly in time. In this case the fixed moment neglects an important degree of freedom in the material and is in most cases a poor approximation. This is most evident in heavy metals such as Pt which has a relatively strong induced moment due to the magnetic proximity effect, where a nearby magnetic atom induces a net moment due to the exchange interaction (Mryasov et al. 2005). Ni also shows some Stoner-like behavior that is not particularly well represented by a fixed spin approximation. However, models of variable spin are much more computationally expensive and so are not currently as widely applicable as standard spin dynamics. In the future models that can better deal with these induced moments will be needed to better understand their behavior.

7 Conclusion

Spin dynamics is becoming a standard research method in the field of magnetism and spintronics due to the ability to model a diverse range of magnetic materials and phenomena, with an increasing ability to be predictive. Through a combination of advanced materials modeling of the structure of materials, their complex magnetic interactions, and spin dynamics simulations, it is now possible to model a wide range of magnetic phenomena which were poorly understood only 20 years ago. This rapidly developing capability will complement ongoing experimental efforts to make devices for a range of practical applications.

Acknowledgments The author is grateful for financial support from the European Materials Modelling Council (EMMC) funded under the European Union's Horizon 2020 research and innovation program under Grant Agreement No 723867.

References

Antropov VP, Katsnelson MI, van Schilfgaarde M, Harmon BN (1995) *Ab Initio*. Phys Rev Lett 75:729–732. https://doi.org/10.1103/PhysRevLett.75.729

Atxitia U, Ostler T, Barker J, Evans RFL, Chantrell RW, Chubykalo-Fesenko O (2013) Ultrafast dynamical path for the switching of a ferrimagnet after femtosecond heating. Phys Rev B 87(22):224417. http://prb.aps.org/abstract/PRB/v87/i22/e224417

Barker J, Bauer GEW (2016) Thermal spin dynamics of yttrium iron garnet. Phys Rev Lett 117:217201. https://doi.org/10.1103/PhysRevLett.117.217201

Barker J, Chantrell RW (2015) Higher-order exchange interactions leading to metamagnetism in FeRh. Phys Rev B 92:094402. https://doi.org/10.1103/PhysRevB.92.094402

Beaurepaire E, Merle JC, Daunois A, Bigot JY (1996) Ultrafast spin dynamics in ferromagnetic nickel. Phys Rev Lett 76:4250–4253. https://doi.org/10.1103/PhysRevLett.76.4250

Bergqvist L, Bergman A (2018) Realistic finite temperature simulations of magnetic systems using quantum statistics. Phys Rev Mater 2:013802. https://doi.org/10.1103/PhysRevMaterials.2.013802

Binder K (1969) A Monte-Carlo method for the calculation of the magnetization of the classical Heisenberg model. Phys Lett A 30(5):273–274. http://www.sciencedirect.com/science/article/pii/037596016990989X

Brown WF (1963) Thermal fluctuations of a single-domain particle. Phys Rev 130(5):1677–1686. https://doi.org/10.1103/PhysRev.130.1677

Callen HB, Callen E (1966) The present status of the temperature dependence of magnetocrystalline anisotropy, and the l(l+1)2 power law. J Phys Chem Solids 27(8):1271–1285. http://www.sciencedirect.com/science/article/pii/0022369766900126

Dzyaloshinsky I (1958) A thermodynamic theory of weak ferromagnetism of antiferromagnetics. J Phys Chem Solids 4(4):241–255. https://doi.org/10.1016/0022-3697(58)90076-3, http://www.sciencedirect.com/science/article/pii/002236975890%0763

Ellis MOA, Evans RFL, Ostler TA, Barker J, Atxitia U, Chubykalo-Fesenko O, Chantrell RW (2015) The Landau-Lifshitz equation in atomistic models. Low Temp Phys 41(9):705–712. https://doi.org/10.1063/1.4930971

Evans RFL, Fan WJ, Chureemart P, Ostler TA, Ellis MOA, Chantrell RW (2014) Atomistic spin model simulations of magnetic nanomaterials. J Phys Condens Matter 26:103202

Evans RFL, Atxitia U, Chantrell RW (2015) Quantitative simulation of temperature-dependent magnetization dynamics and equilibrium properties of elemental ferromagnets. Phys Rev B 91:144425. https://doi.org/10.1103/PhysRevB.91.144425

Fidler J, Schrefl T (2000) Micromagnetic modelling – the current state of the art. J Phys D Appl Phys 33(15):R135. http://stacks.iop.org/0022-3727/33/i=15/a=201

Garanin DA (2017) Pulse-noise approach for classical spin systems. Phys Rev E 95:013306. https://doi.org/10.1103/PhysRevE.95.013306

García-Palacios JL, Lázaro FJ (1998) Langevin-dynamics study of the dynamical properties of small magnetic particles. Phys Rev B 58:14937–14958. https://doi.org/10.1103/PhysRevB.58.14937

Gerlach W, Stern O (1924) Der experimentelle Nachweis der Richtungsquantelung im Magnetfeld. Zeitschrift für Physik 9(1):349–352

Gilbert TL (1955) A Lagrangian formulation of the gyromagnetic equation of the magnetic field. Phys Rev 100:1243. https://doi.org/10.1103/PhysRevB.100.1235

Heisenberg W (1928) Zur theorie des ferromagnetismus. Z Phys 49:619

Ising E (1925) Contribution to the theory of ferromagnetism. Z Phys 31:253–258

Kirilyuk A, Kimel AV, Rasing T (2010) Ultrafast optical manipulation of magnetic order. Rev Mod Phys 82:2731–2784. https://doi.org/10.1103/RevModPhys.82.2731

Krech M, Bunker A, Landau D (1998) Fast spin dynamics algorithms for classical spin systems. Comput Phys Commun 111(1):1–13. http://www.sciencedirect.com/science/article/pii/S0010465598000095

Landau LD, Lifshitz EM (1935) Theory of the dispersion of magnetic permeability in ferromagnetic bodies. Phys Z Sowietunion 8:153

Ma PW, Woo CH, Dudarev SL (2008) Large-scale simulation of the spin-lattice dynamics in ferromagnetic iron. Phys Rev B 78:024434. https://doi.org/10.1103/PhysRevB.78.024434

Metropolis N, Rosenbluth AW, Rosenbluth MN, Teller AH, Teller E (1953) Equation of state calculations by fast computing machines. J Chem Phys 21(6):1087. https://doi.org/10.1063/1.1699114

Moriya T (1960) Anisotropic superexchange interaction and weak ferromagnetism. Phys Rev 120:91–98. https://doi.org/10.1103/PhysRev.120.91

Mryasov ON, Nowak U, Guslienko KY, Chantrell RW (2005) Temperature-dependent magnetic properties of fept: effective spin hamiltonian model. Euro Phys Lett 69(5):805. http://stacks.iop.org/0295-5075/69/i=5/a=805

Nedelkoski Z, Kepaptsoglou D, Lari L, Wen T, Booth RA, Oberdick SD, Galindo PL, Ramasse QM, Evans RFL, Majetich S et al (2017) Origin of reduced magnetization and domain formation

in small magnetite nanoparticles. Sci Rep 7. https://doi.org/10.1038/srep45997, http://www.osti.gov/pages/servlets/purl/1366451

Nowak U (2007) Classical spin models. Wiley. https://doi.org/10.1002/9780470022184.hmm205

Ostler TA, Evans RFL, Chantrell RW, Atxitia U, Chubykalo-Fesenko O, Radu I, Abrudan R, Radu F, Tsukamoto A, Itoh A, Kirilyuk A, Rasing T, Kimel A (2011) Crystallographically amorphous ferrimagnetic alloys: comparing a localized atomistic spin model with experiments. Phys Rev B 84:024407. https://doi.org/10.1103/PhysRevB.84.024407

Ostler TA, Barker J, Evans RFL, Chantrell RW, Atxitia U, Chubykalo-Fesenko O, El Moussaoui S, Le Guyader L, Mengotti E, Heyderman LJ, Nolting F, Tsukamoto A, Itoh A, Afanasiev D, Ivanov BA, Kalashnikova AM, Vahaplar K, Mentink J, Kirilyuk A, Rasing T, Kimel AV (2012) Ultrafast heating as a sufficient stimulus for magnetization reversal in a ferrimagnet. Nat Commun 3:666. http://www.nature.com/doifinder/10.1038/ncomms1666

Pan F, Chico J, Hellsvik J, Delin A, Bergman A, Bergqvist L (2016) Systematic study of magnetodynamic properties at finite temperatures in doped permalloy from first-principles calculations. Phys Rev B 94:214410. https://doi.org/10.1103/PhysRevB.94.214410

Pan F, Chico J, Delin A, Bergman A, Bergqvist L (2017) Extended spin model in atomistic simulations of alloys. Phys Rev B 95:184432. https://doi.org/10.1103/PhysRevB.95.184432

Perera D, Eisenbach M, Nicholson DM, Stocks GM, Landau DP (2016) Reinventing atomistic magnetic simulations with spin-orbit coupling. Phys Rev B 93:060402. https://doi.org/10.1103/PhysRevB.93.060402

Perera D, Nicholson DM, Eisenbach M, Stocks GM, Landau DP (2017) Collective dynamics in atomistic models with coupled translational and spin degrees of freedom. Phys Rev B 95:014431. https://doi.org/10.1103/PhysRevB.95.014431

Radu I, Vahaplar K, Stamm C, Kachel T, Pontius N, Dürr HA, Ostler TA, Barker J, Evans RFL, Chantrell RW, Tsukamoto A, Itoh A, Kirilyuk A, Rasing T, Kimel AV (2011) Transient ferromagnetic-like state mediating ultrafast reversal of antiferromagnetically coupled spins. Nature 472(7342):205–208. http://www.nature.com/doifinder/10.1038/nature09901

Simoni J, Stamenova M, Sanvito S (2017) Ultrafast demagnetizing fields from first principles. Phys Rev B 95:024412. https://doi.org/10.1103/PhysRevB.95.024412

Skomski R (2012) Simple models of magnetism. OUP, Oxford

Skubic B, Hellsvik J, Nordström L, Eriksson O (2008) A method for atomistic spin dynamics simulations: implementation and examples. J Phys Condens Matter 20(31):315203. https://doi.org/10.1088/0953-8984/20/31/315203, http://stacks.iop.org/0953-8984/20/i=31/a=315203?key=crossref.74bd3abd0f58484825bcbd4af5661ec8

Stanciu CD, Hansteen F, Kimel AV, Kirilyuk A, Tsukamoto A, Itoh A, Rasing T (2007) All-optical magnetic recording with circularly polarized light. Phys Rev Lett 99:047601. https://doi.org/10.1103/PhysRevLett.99.047601

Szunyogh L, Lazarovits B, Udvardi L, Jackson J, Nowak U (2009) Giant magnetic anisotropy of the bulk antiferromagnets IrMn and $IrMn_3$ from first principles. Phys Rev B 79:020403. https://doi.org/10.1103/PhysRevB.79.020403

Toga Y, Matsumoto M, Miyashita S, Akai H, Doi S, Miyake T, Sakuma A (2016) Monte Carlo analysis for finite-temperature magnetism of $Nd_2Fe_{14}B$ permanent magnet. Phys Rev B 94:174433. https://doi.org/10.1103/PhysRevB.94.174433

Weiss P (1907) L'hypothèse du champ moléculaire et la propriété ferromagnétique. J Phys Theor Appl 1:661–690. https://doi.org/10.1051/jphystap:019070060066100

Yanes R, Chubykalo-Fesenko O, Kachkachi H, Garanin DA, Evans R, Chantrell RW (2007) Effective anisotropies and energy barriers of magnetic nanoparticles with néel surface anisotropy. Phys Rev B 76:064416. https://doi.org/10.1103/PhysRevB.76.064416

Yanes R, Jackson J, Udvardi L, Szunyogh L, Nowak U (2013) Exchange bias driven by Dzyaloshinskii-Moriya interactions. Phys Rev Lett 111:217202. https://doi.org/10.1103/PhysRevLett.111.217202

Yang Y, Wilson RB, Gorchon J, Lambert CH, Salahuddin S, Bokor J (2017) Ultrafast magnetization reversal by picosecond electrical pulses. Sci Adv 3(11):e1603117. http://advances.sciencemag.org/content/3/11/e1603117